1

MIXTURE LAWS AND MICROWAVE-MATERIAL INTERACTIONS

W. R. Tinga

1.1 Introduction

What makes the dielectric properties of materials so important? It is because, electromagnetic (EM) energy transformation, whether it

occurs reversibly or irreversibly, is always the result of the interaction of EM waves with actual materials. Therefore, the study of the dielectric and magnetic properties of heterogenous mixtures is an area of very practical significance. Increasing use of EM energy for industrial processing, medical use, non-destructive testing, geophysical mapping and remote sensing makes it mandatory to know how to predict a material's or system's effective dielectric and magnetic properties and the internal, localized EM fields. Fortunately, field intensity, dielectric or magnetic properties and EM heating rate calculations are very closely related.

For that reason, Section 1.2 reviews the historic basis of dielectric mixture theory and its validity for practical applications and later sections address the fundamental principles of microwave material interactions in some detail including microwave heating models and their application. Eventhough the discussion in Sections 1.3, 1.4, 1.5 and 1.6 centers around microwave heating, the principles and equations hold for all EM frequencies as long as the basic assumptions of the theory are met. The treatment given here is intended to give physical insight into the EM material interaction phenomena without going into rigorous mathematical details. Adequate references are given to pursue the topics in greater depth.

1.2 Dielectric Mixture Theory

Given a mixture made up of different components, each with its own dielectric and shape characteristics, can the dielectric behavior of the mixture as a whole be predicted? To answer this problem, dielectric mixture theory was developed as far back as 1891 when Maxwell [1] tackled the problem of obtaining the electromagnetic characteristics of simple magnetic mixtures. Since that time, many researchers have modified, added to, and improved on the early theories [2,3,4,5,6,7,8]. An exact solution of the problem is possible for only a few idealized and geometrically well-defined systems. For many natural materials, the geometries of the mixture components and the interaction between the components can be described approximately at best. Nevertheless, much work has recently been done on discrete scatterers and random continuous media with the help of classical and modern approaches to predict mixture behavior with reasonable success [9,10]. Elsewhere in

this book there is ample evidence of these approaches.

1.2.1 Qualitative Overview

Space does not allow the listing of all the mixture relations developed over the years nor would that be all that helpful since De Loor [7], Böttcher [11], Van Beek [2] and, recently, Sihvola [6] have all critically reviewed portions of the literature on dielectric mixtures. In Table 1.1, a list of the major classical mixture theories are given from which most of the others can be derived.

To facilitate this introductory discussion on mixture theory, some fundamental relationships are reviewed. Consider the rather simple, idealized representation of a multiphase mixture shown in Fig. 1.1. Now isolate one of the inclusions as shown in Fig. 1.2. The polarizable inclusion is assumed to exist in a homogeneous host material. When an average macroscopic field, $\overline{E}$, is excited in this heterogeneous mixture, it will induce polarization in the inclusion which, by definition, is related to the displacement or electric flux density, $\overline{D}$, by

$$\overline{D} = \varepsilon_h \overline{E} + \overline{P} \tag{1}$$

where ε_h is the permittivity of the host material and the polarization, $\overline{P}$, depends on n, the number of polarizable particles per unit volume, their polarizability, α, and the 'local' electric field, $\overline{E_L}$, at the inclusion boundary.

$$\overline{P} = n\alpha \overline{E}_L \tag{2}$$

But the macroscopic behavior of the included material itself is also given by

$$\overline{D}_{ave} = \varepsilon_i \overline{E}_{ave} \tag{3}$$

where ε_i refers to the macroscopic dielectric constant of the inclusion material and $\overline{D}_{ave}$ and $\overline{E}_{ave}$ are the averaged fields. Combining (1), (2) and (3) defines the polarizability for n inclusions as

$$n\alpha = (\varepsilon_i - \varepsilon_h)\frac{\overline{E}_{ave}}{\overline{E}_L} \tag{4}$$

It is the calculation of the field ratio in (4) which is the key to solving the mixture problem using the effective media approach.

Author, mixture, comments	Mixture formula
1.) Maxwell, 1891 [1] spheres, 2-phase Maxwell-Garnett formula; identical to Rayleigh's results.* $\epsilon_a = \epsilon_h$ (see footnote)	$\epsilon = \epsilon_h + \frac{3V_i\epsilon_h}{[(\epsilon_i+2\epsilon_h)/(\epsilon_i-\epsilon_h)]-V_i}$
2.) Rayleigh, 1892 [13] spheres, 2-phase; $\epsilon_a = \epsilon_h$	$\frac{\epsilon-\epsilon_h}{\epsilon+2\epsilon_h} = V_i\left(\frac{\epsilon_i-\epsilon_h}{\epsilon_i+2\epsilon_h}\right)$
3.) Wiener, 1912 [15] arbitrary shape, 2-phase; $\epsilon_a = \epsilon_h$; u = form factor; $u = 2\epsilon_h$ for spheres (Rayleigh form); $u = 2\epsilon_i$ = disks $u = \frac{1}{2}(\epsilon_i - 3\epsilon_h)$ = needles.	$\frac{\epsilon-\epsilon_h}{\epsilon+u} = V_i\left(\frac{\epsilon_i-\epsilon_h}{\epsilon_i+u}\right)$
4.) Bruggemann, 1935 [16] spheres, 2-phase; $\epsilon_a = \epsilon$; $\left(a = \frac{2}{3}\right)$	$\frac{\epsilon_i-\epsilon}{\epsilon_i-\epsilon_h} = (1-V_i)\left(\frac{\epsilon}{\epsilon_h}\right)^{\frac{1}{3}}$
5.) Böttcher, 1945 [11] spheres, 2-phase $\epsilon_a = \epsilon$	$\frac{\epsilon-\epsilon_h}{3\epsilon} = V_i\left(\frac{\epsilon_i-\epsilon_h}{\epsilon_i+2\epsilon}\right)$
6.) Polder, van Santen, 1946 [27] ellipsoids, multiphase; $\epsilon_a = \epsilon$, $(a = 1-N_i)$ see also Tinga [4] for shell inclusions DeLoor [7], Sihvola, Kong [6]	$\epsilon - \epsilon_h = \sum_{i=1}^{N} V_i(\epsilon_i - \epsilon_h)\frac{E_{int}}{E_{ave}}$ where $\frac{E_{int}}{E_{ave}} = \frac{1}{3}\sum_{j=1}^{3}\left[1 + N_j\left(\frac{\epsilon_i}{\epsilon} - 1\right)\right]^{-1}$
7.) Looyenga, 1965 [18] spheres, 2-phase	$\epsilon^{\frac{1}{3}} = V_i\epsilon_i^{\frac{1}{3}} + (1-V_i)\epsilon_h^{\frac{1}{3}}$
8.) Sihvola, Kong, 1988 [6] ellipsoids, random orientation	$\epsilon = \epsilon_h + \sum_{i=1}^{3}\frac{V(\epsilon_i-\epsilon_h)[\epsilon_a+N_i(\epsilon-\epsilon_h)]}{3[\epsilon_a+N_i(\epsilon_i-\epsilon_h)]}$ where $\epsilon_a = \epsilon_h + a(\epsilon - \epsilon_h)$ OR $\epsilon = \epsilon_h + \frac{\sum_{i=1}^{3}\frac{V\epsilon_a(\epsilon_i-\epsilon_h)}{3[\epsilon_a+N_i(\epsilon_i-\epsilon_h)]}}{1-\sum_{i=1}^{3}\frac{VN_i(\epsilon_i-\epsilon_h)}{3[\epsilon_a+N_i(\epsilon_i-\epsilon_h)]}}$

* Apparent permittivity as defined by Sihvola, Kong [6]: $\epsilon_a = \epsilon_h + a(\epsilon_{eff} - \epsilon)$; $0 \le a \le 1$. If $a = 0$, generalized Maxwell-Garnett or Rayleigh form results. If $a = 1$, Coherent Potential Approximation (CPA) is obtained. If $a = 1 - N_i$, (for spheres $a = \frac{2}{3}$) the Polder van Santen case, is recovered. ϵ_h = host or background permittivity; ϵ_i = inclusion or scatterer permittivity; ϵ = effective mixture permittivity; N_j = depolarization coefficient; V, V_i = fractional inclusion volume

Table 1.1 Summary of major mixture formulas.

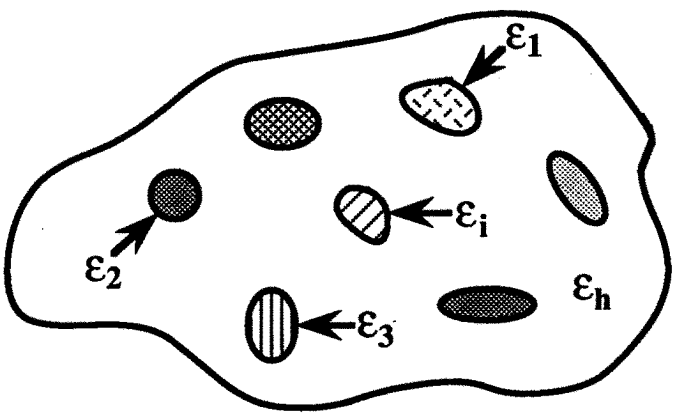

Figure 1.1 Multiphase mixture representation.

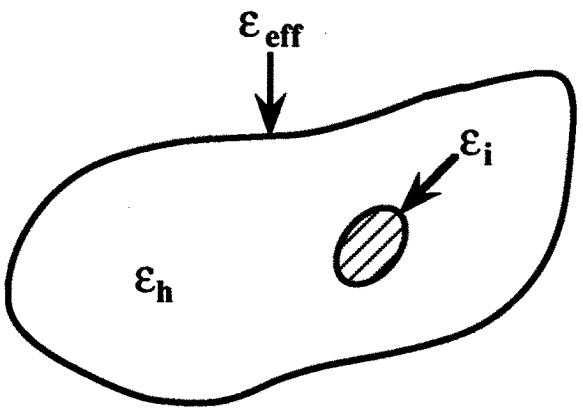

Figure 1.2 Isolated inclusion in an effective medium.

More generally, the ratio of the average $\overline{D}$ and $\overline{E}$ fields defines the effective permittivity of the mixture.

$$\overline{D}_{ave} = \varepsilon_{eff}\overline{E}_{ave} \tag{5}$$

Then using (2) and (5) in (1) yields

$$\varepsilon_{eff}\overline{E}_{ave} = \varepsilon_h\overline{E}_{ave} + n\alpha\overline{E}_L \tag{6}$$

hence

$$\varepsilon_{eff} = \varepsilon_h + n\alpha\frac{\overline{E}_L}{\overline{E}_{ave}} \tag{7}$$

In a very general manner, Yaghjian [12] shows, that for an arbitrarily shaped inclusion the local field is given as

$$\overline{E}_L = \overline{E}_{ave} + \frac{\overline{\overline{L}}\cdot\overline{P}}{\varepsilon^*} \tag{8}$$

where $\overline{\overline{L}}$ is called a source dyadic which depends only on the geometry of the source region, and ε^* is the value of the permittivity just outside the inclusion. In our case, the source region is the inclusion acting as an equivalent dipole. Yaghjian says that "this dyadic for an arbitrary inclusion size and time harmonic fields" can be interpreted as a generalized depolarizing dyadic. Now substitute (2) in (8) to get

$$\overline{E}_L = \overline{E}_{ave} + \frac{\overline{\overline{L}}\cdot n\alpha\overline{E}_L}{\varepsilon^*} \tag{9}$$

Since the trace of $\overline{\overline{L}}$ is unity [12], $\overline{\overline{L}}$ can always be found in terms of only two independent quantities, e.g., given L_{xx}, L_{yy}, then the third is $L_{zz} = 1 - L_{xx} - L_{yy}$. If all inclusions have the same shape and have principal axes in the same direction, then one can solve for the local (internal) to average (external) field ratio from (9). For example,

$$\frac{\overline{E}_L}{\overline{E}_{ave}} = \left[1 - \frac{L_{xx}n\alpha_x}{\varepsilon^*}\right]^{-1} \tag{10}$$

and use it in (7) to obtain

$$\varepsilon_{eff_x} = \varepsilon_h + \frac{\dfrac{n\alpha_x}{1 - L_{xx}n\alpha_x}}{\varepsilon_h} \tag{11}$$

Therefore, to obtain the mixture permittivity it is necessary to calculate the polarizability, α, of an inclusion which requires calculating the local to average field ratio. Sihvola, in a recent paper [6], has generalized the above analysis for different discrete ellipsoidal inclusion shapes in isotropic and anisotropic mixtures. Continuous (non-discrete) inclusions with variable permittivity profiles can be handled by his method as well. Considerable detail on this methodology is covered by Sihvola [9].

One must conclude that the local or exciting field, discussed a bove, can be approximated by the average macroscopic field only when the inclusions are far enough apart so that the polarizing field of one inclusion does not substantially affect the macroscopic field at a neighboring inclusion. In fact, as (9) shows, the exciting or local field for a given inclusion must be the sum of the average macroscopic field plus the depolarization field of the inclusion itself.

From this point of view, two distinct approaches to solving mixture problems have emerged and can be summarized as follows:

1. Calculate the internal to external electric field ratio for the volume of a single inclusion placed in a material with an effective permittivity, to yield the inclusion polarization and hence the mixture permittivity by appropriate summation or integration.
2. Calculate the perturbation effect of an inclusion's effective dipole on the field external to the inclusion and from it determine the dipole strength, the inclusion's polarization and finally the mixture permittivity.

It is therefore, necessary with the first approach to calculate the field internal to an inclusion which in the quasi-static case means the solving of Laplace's equation. Any solution to such a problem must involve the inclusion geometry. Both approaches, if executed correctly, should yield the same results. The choice and suitability of either method, as Sihvola [9] clearly demonstrates, depends on convenience and the assumed permittivity profile. Moreover, both methods give internal to external field ratio information which is directly applicable in predicting EM heating performance of a material at a localized level as will be shown in Section 1.4.2. In either method, the geometrical shape and orientation of the particle must be specified, which in practice, is always a guess or approximation at best. Inclusion size is accounted for through a fractional volume parameter.

Having given a review of how dielectric constants for mixtures

can be estimated, let us briefly survey the classical methods. Discrete inclusions are assumed in all of the classical theories. Only recently have random continuous media been modelled using the internal field calculation method [9] and a renewed effort at applying scattering theory along with correlation functions [10] is being made. In all cases, the largest particle dimension is assumed to be much less than a wavelength so that scattering losses can be neglected.

1.2.2 Classical Mixture Relations - A Summary

The main features and assumptions of some of the common classical mixture relations are described below with the actual mixture model formulas summarized in Table I.

Neglecting all particle interactions, Maxwell [1] treated the problem of anisotropic ellipsoidal inclusions in an isotropic magnetic medi um. The well-known Maxwell-Garnett Theory (MGT) assumes the microstructure of a material to be that of an infinite homogeneous host material, ε_h, with one inclusion phase, ε_i, which is a non self-consistent but still useful treatment of the mixture. The MGT gives the resultant mixture permittivity, ε, simply and directly.

Rayleigh [13] showed that the Maxwell model is a good first order approximation for cubically arranged spherical and cylindrical inclusions in a host material.

Rayleigh's equation is just a simpler but entirely equivalent form of the MGT. Cohen, et al. [14], Sihvola, et al. [6] and others have generalized the MGT for non-spherical inclusions. Cohen, et al. [14] note that the MGT breaks down around the percolation threshold because of the resultant host matrix inversion.

Wiener [15] derived a semi-empirical formula which relies on a "formzahl" (form number). Bruggeman [7,11,16] showed Wiener's "formzahl" to be a function of the dielectric constants of the host and the mixture. It can readily be shown that Wiener's form number U equals $2\varepsilon_h$ for spheres, and hence Rayleigh's formula is recovered. In general, the form number is related to the shape or depolarization factor of the inclusions (see Table I). Both Bruggeman and Böttcher [11,16] attempted to improve on Maxwell's theory by allowing for long-range interactions via a limit or differential procedure. Niesel [17] arrived at Bruggeman's results by using an integration process and the same results have been independently deduced by Looyenga [18,19].

It was Bruggeman who first formulated an effective medium the-

ory (EMT) for mixtures. In general, the EMT allows for the fact that the 'apparent' permittivity, ε_a, surrounding the inclusion is different from that of the host. Bruggeman assumed $\varepsilon_a = \varepsilon_{eff}$. Sihvola and Kong [6] give a concise generalization of the relations resulting from the many different assumptions regarding this localized apparent permittivity. Whenever the assumed ε_a is greater than ε_h, (host or background material), a nonlinear equation for mixture permittivity results in contrast to the linear MGT. Stroud, [20] among others, indicates that the EMT is "a loose analog of the coherent potential approximation (CPA)" used in alloy theory whereas the MGT and other non-self-consistent mixture theories are the analogs of the average matrix approximation (ATA) of alloy theory. He further generalized the effective medium approach for an inhomogeneous material.

In a manner different from Brown's statistical treatment [21], Sihvola [6] shows, that the Bruggeman formula, when applied to dense mixtures with spherical inclusions, is valid to the second order. This formula has consistently given good results in many different applications. For example, Nelson [22, 23] shows that experimental data on granular materials as a function of density show very good correlation to Bruggeman's formula and on this basis predicts the permittivity of the actual solid material.

Lewin [24] applied scattering theory and allowed for particle interaction by defining an effective dielectric constant as a complex function of particle size and the properties of the spherical inclusions (small compared to a wavelength). Lewin's model equation for spheres is identical to the Maxwell-Garnett relation. Lichtenecker [25] gives an empirical formula which shows little correlation to any of the previous theories but the logarithmic model used was referenced by Brown [21].

In 1936, Onsager [26] first proposed that only a part of the internal field in a mixture is effective in directing a dipole. He introduced a reaction field which accounts for long range interaction effects. Böttcher [11] used this approach to derive a relation for a 2-phase spherical inclusion mixture. This approach was later generalized by Polder and van Santen [27] for ellipsoidal inclusions of more than one material and assuming $\varepsilon_a = \varepsilon_{eff}$. They also showed that Onsager's assumptions about the reaction field were equivalent to the hypothesis that: "the mean value of the field in the interior of a particle of dielectric constant ε_i surrounded by a medium of dielectric constant ε' in which a homogeneous field E_{ave} is maintained at large distances from the par-

ticle, is a good approximation for the actual mean field in this special particle".

De Loor [7] further modified Polder and van Santen's approach by assigning an effective dielectric constant, ε^*, to the immediate surroundings of an included particle. This apparent ε^*, in effect, models the short-range interaction between the isolated inclusion being studied and its near neighbors which is necessary if the theory is to hold for dense mixtures. However, according to Sihvola, "DeLoor's formula is not valid for high fractional volume... unless the choice $\varepsilon^* = \varepsilon_{eff}$ is made, in which case it reduces to the Polder-vanSanten formula." [6]

Generalized mixture relations can also be derived via vector calculus from Maxwell's equations. Taylor [28] used Polder and van Santen's average field approximation to arrive at generalized equations for lossy anisotropic media. His very concise development is based on work by Korneenko [29] and Franck [30]. The theoretical treatment of fields in source regions by Yaghjian [12] uses a similar but even more general methodology.

Both Kirkwood [31] and Brown [21] developed statistical methods in an attempt to solve the particle interaction, or modified 'local' field problem. For example, Brown shows that the Bruggeman and Böttcher formulas agree to the second order of small quantities. In their approximations, statistical properties of particle geometry have been neglected. Brown further argues that improving on the simpler averaging formulas requires a correction term which is independent of the inclusion geometry. This claim seems reasonable since the improvement has to come from a correction to the neglected modified local field outside of the inclusions.

1.2.3 Effective Permittivity - Its Validity

The method of effective permittivity, so commonly used, is valid when the fields can be considered as quasi-static. This is the case when the absolute value of the product of propagation constant and a typical distance in the mixture is much less than unity [12, 19].

Most of the classical mixture relations work reasonably well for dilute mixtures, volume fraction less than 10%, but fail to predict accurately the mixture behavior when the inclusion density is higher as is the case in many practical situations. The Bruggeman formula, is based on a 'self similar' mixture argument and is shown to fit remarkably well even for non-dilute mixture cases [6,23]. The multiphase theory of

Tinga et al. [4], based on a self-consistent internal field approach, also gives good results even for non-dilute mixtures with ellipsoidal shell inclusions. Self-consistency implies that ε_{eff} is position independent and that the average of all local field variations over the medium equal zero. All these theories assume random discrete media. Nevertheless, such effective medium theories fail when the "percolation point" is reached in a mixture or when there is no longer a true randomness.

Sihvola and Kong [6,9] give a systematic approach to developing self-consistent mixture relations using both the internal and external field approaches. They also show that most of the non- self-consistent mixture relations can be cast into a generalized Rayleigh or Maxwell-Garnett form which gives the mixture's effective permittivity directly as a function of partial filling factors, particle geometry, anisotropy and inclusion permittivities. Their work extends the mixture equations to multilayer shells and non-discrete, random media with nonlinear permittivity variations.

It is interesting to observe that most of the classical mixture relations give similar results as long as the inclusion to host permittivity contrast is low. As this contrast ratio increases, the results from the various mixture relations diverge indicating the differences in the fundamental assumptions made about the polarizing local fields. A similar argument holds when the inclusion to host volume density increases to above 10 %.

For example, Tsang and Kong [32] show by scattering theory that, for large contrast ratios (> 10) between the background medium and the random scattering inclusions, the effective complex permittivity is considerably different from the weak fluctuation (low contrast ratio) theory result even at low scatterer density. Because of the low scatterer density, the scatterer's dielectric loss factor plays a major role in the effective scattering cross section.

Nearest neighbor interactions in an effective medium are treated by Sheng [33] using a "pair-cluster" theory. He notes that the effective medium theory (EMT) originated by Bruggeman and the Maxwell-Garnett Theory (MGT) basically treat two different microstructures. "Whereas in the EMT the two components are treated in an equivalent manner, in the MGT the grains of one component are taken to be embedded in the matrix of the other component." However, the classical EMT approximation neglects nearest neighbor interactions between the two components. Sheng also notes that the EMT perco-

lation threshold occurs at a fractional volume of 0.33 but that this percolation threshold, and therefore the DC transport behavior, such as conductivity, is not greatly affected by nearest neighbor interactions.

The virtue of the EMT is that it is applicable, except near the percolation threshold, to high volume filling factor mixtures despite its neglect of near neighbor effects. Neglect of these effects naturally reduces the theory's accuracy, especially for the case of high permittivity contrast ratios.

Multi-scattering theory, when combined with correlation functions, appears to hold promise of predicting mixture properties in the more general cases of non-random, non-dilute mixtures [10]. However this approach is computationally very complex and still requires many assumptions about the statistical nature and geometry of the inclusions. Nonetheless, using this approach, Varadan [10] showed that, in sintering ceramics, there is a critical concentration (near 50% porosity) at which the loss factor of a mixture attains a maximum value. It is also at this concentration that maximum heating rate is achieved. This critical concentration depends on the material properties but appears to be more dependent on the matrix-host geometry and percolation threshold. For example, Varadan's results agree with the work of Cohen et al. [14] which showed a strong variation of conductivity near the 50% composition point in metal-insulator mixtures.

The difficulty of calculating the correct shapes and fields in an arbitrary material will always limit the accuracy of even the best mixture theories especially near the percolation point. Nevertheless, their usefulness outweighs their limitations in most cases. As will be shown later, localized heating rates at the particle level can be calculated from the field ratios obtained from a mixture model.

In order to establish the heating rate relationships and because of the varying backgrounds of readers, it may be helpful to briefly review some aspects of wave propagation and the basic EM energy conservation theorem.

1.3 Microwave Interactions with Practical Materials

Microwave (MW) energy, when incident on a material, creates heating within the material through the interaction of the electromagnetic force fields with the materials' molecular and electronic struc-

ture. As a result, MW energy sources have low thermal inertia and, by appropriate design of the MW-material interface, energy deposition is both reasonably predictable and controllable. Ionic conduction, ion jumping, and dipole reorientation are the major mechanisms causing MW heating at the ISM (Industrial, Scientific and Medical) frequencies for which commercial power sources are available, e.g., 915, 2450 MHz,. Activation energies of certain rate processes such as sintering and diffusion also appear to be altered by the applied EM energy.

As has been shown in the previous section, applying external EM fields to a material mixture, has the immediate electromagnetic consequence that the EM waves come across a variety of microscopic boundary conditions due to the inclusions making up the mixture. The resulting local field variations can have a very strong effect on energy absorption at such boundaries since absorption always depends on the square of the electric field intensity. In this section the EM heating equations and macroscopic boundary conditions, as determined by bulk shape and size, will be considered.

1.3.1 Electromagnetic Energy Absorption

The 3-dimensional wave equation for the electric, E, or magnetic, H, fields yields solutions which are dependent on the space, time and material property variables. For example,

$$\overline{E} = f(x, y, z, t, \rho, \varepsilon, \mu) \tag{12}$$

For a wave propagating in the positive z-direction,

$$\overline{E} = \overline{E}_o e^{-\gamma z}$$

where the propagation factor, γ , is determined strictly by the material properties at a given frequency and temperature and is defined as

$$\gamma = j\omega\sqrt{\mu\varepsilon} = \alpha + j\beta \tag{13}$$

where α = the attenuation constant in nepers /m = $Re(j\omega\sqrt{\mu\varepsilon})$ and β = the phase constant in radians/s = $Im(j\omega\sqrt{\mu\varepsilon})$ and

$$\varepsilon = \varepsilon' - j\varepsilon''$$

$$\tan\delta_e = \varepsilon''/\varepsilon'$$

$$\mu = \mu' - j\mu''$$

$$\tan \delta_\mu = \mu''/\mu'$$

Unfortunately, the material properties ε and μ depend on many variables also. For example, $\varepsilon = g\ (T, f, \rho, x, y, z$, composition) where T is the temperature, f is the frequency and ρ is the density.

Energy loss in a material illuminated by EM waves comes about through damping forces acting on polarized atoms and molecules and through the finite conductivity of a material. An electromagnetic energy balance equation, known as the complex Poynting vector theorem, may be written from Maxwell's equations using vector calculus. This relation equates power flow, into a volume V through a closed surface S, to the EM fields and material properties within the volume. The real power flowing in through such a surface is the dissipated or absorbed power and is given as [34]

$$\begin{aligned} P_{diss} &= Re\left\{\frac{1}{2}\oint_s (\overline{E} \times \overline{H}^*) \cdot (-d\overline{S})\right\} \\ &= \frac{\omega}{4}\int_v \left(\mu''\overline{H}\cdot\overline{H}^* + \varepsilon''\overline{E}\cdot\overline{E}^* + \frac{\sigma}{\omega}\overline{E}\cdot\overline{E}^*\right) dv \end{aligned} \tag{14}$$

where RMS field amplitudes are assumed and convection currents (e.g., plasmas) and free charge distributions are not accounted for. The result is, however, valid for dispersive or non-dispersive media.

It is apparent that conductivity and the magnetic and dielectric loss factors are directly responsible for the energy dissipation. Without loss of generality, non-magnetic materials are assumed from here on and so (14) reduces to

$$P_{diss} = \frac{1}{4}\int_v (\sigma + \omega\varepsilon'')\left|\overline{E}\right|^2 dv \tag{15}$$

The conductive and dielectric loss mechanisms are, however, indistinguishable with respect to any heat generated. Therefore, one can define an effective dielectric loss factor

$$\varepsilon_e'' = \varepsilon'' + \frac{\sigma}{\omega} \tag{16}$$

or equally, a total effective conductivity can be defined as

$$\sigma_e = \omega\varepsilon'' + \sigma_d \tag{17}$$

where σ_d is the conductivity of the dielectric material. Note that absolute values of the dielectric constants are used in the above. In the limit of an infinitesimal volume, (15) can be written as a differential relation giving the power density at a point,

$$\frac{dP_{diss}}{dv} = \frac{1}{4}(\sigma + \omega\varepsilon'')\left|\overline{E}\right|^2 = \frac{1}{4}\omega\varepsilon_e''\left|\overline{E}\right|^2 \tag{18}$$

This equation is often misused by applying it to finite volumes and using a given E-field at a particular point within that volume. It must be stressed that only total power dissipation in a volume, not the power density at a point, can be evaluated experimentally.

1.3.2 Electromagnetic Boundary Conditions

Apart from the microscopic boundaries encountered in a dielectric mixture, the EM waves need to obey macroscopic boundary conditions set by the physical form of the material as the waves see it.

1.3.2.1 Uniform Plane Wave Systems

The reflection coefficient of a nonmagnetic material interface seen by a normally incident uniform plane wave, see Fig. 3, is given by [34]

$$\Gamma = \frac{\overline{E}_r}{\overline{E}_i} = \frac{\sqrt{\varepsilon_1} - \sqrt{\varepsilon_2}}{\sqrt{\varepsilon_1} + \sqrt{\varepsilon_2}} \tag{19}$$

Power transmitted into the second material, assuming no further reflections occur, can then be written as

$$P_t = P_i\left(1 - |\Gamma|^2\right) \tag{20}$$

and at a distance z into the material the power is

$$P_t = P_i\left(1 - |\Gamma|^2\right)e^{-2\alpha z} \tag{21}$$

where

$$\alpha = Re\left\{j\sqrt{\omega^2\mu\varepsilon - \omega_c^2\mu_o\varepsilon_o}\right\}$$

ω_c is the cutoff frequency, in radians, of the propagation medium. If we define

$$p = \left(\frac{\lambda_o}{\lambda_c}\right)^2 = \left(\frac{f_c}{f}\right)^2$$

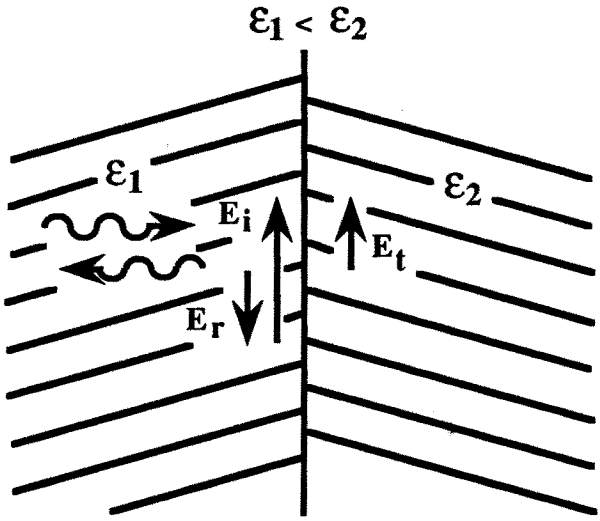

Figure 1.3 Uniform plane wave normally incident on a semi-infinite slab. Power flow is incident from the left. Field magnitudes are continuous across the boundary, that is $E_t = E_i - E_r$.

then

$$\alpha = \omega \sqrt{\varepsilon_o \mu_o \left(\frac{\varepsilon' - p}{2}\right)\left[\sqrt{1 + \frac{\varepsilon''}{\varepsilon' - p}} - 1\right]} \tag{22}$$

For unbounded propagation, $p = 0$.

Electric fields perpendicular to an interface, such as created by oblique incidence of a plane wave on an interface, are discontinuous. This is illustrated schematically in Fig. 1.4. Assuming $\varepsilon_2 > \varepsilon_1$ and $\mu = \mu_o$, then $\varepsilon_1 \overline{E}_1 = \varepsilon_2 \overline{E}_2$ and the power density just to the left of the interface will be, by (18),

$$\frac{dP_{abs_1}}{dV} = \frac{\omega \varepsilon_1''}{4} \left|\overline{E}_1\right|^2 \tag{23}$$

The perpendicular electrical field in medium 2 will be lower than that

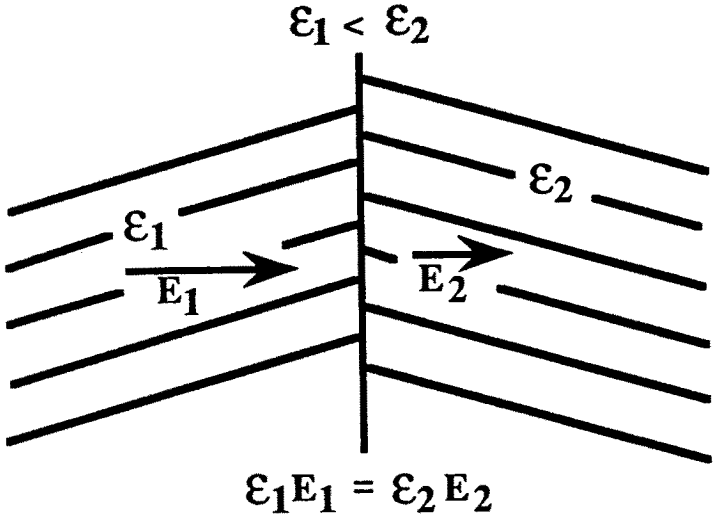

Figure 1.4 Discontinuity of the normal electric field at a boundary betweeen two media when no surface charge resides at the boundary. Field magnitude in the denser medium is always the smaller of the two, that is $\epsilon_1 E_1 = \epsilon_2 E_2$.

in medium 1 by the ratio of dielectric constants and so

$$\frac{dP_{abs_2}}{dv} = \frac{\omega}{4}\left(\frac{\epsilon_1'}{\epsilon_2'}\right)^2 \left(\epsilon_2''\right)\left|\overline{E}_1\right|^2 \tag{24}$$

As a result of this type of polarization, a ratio of 10 in permittivity, across a plane boundary, will cause a factor of 100 difference in power intensity on the two sides even if the effective loss factors are the same.

Similar results can be obtained for microscopic boundaries within a material by applying mixture theory to predict the localized fields, at least in an approximate manner, as illustrated earlier by (10). The mixture theory itself allows for varying field polarization and particle boundary conditions. This application of mixture theory to the power absorption problem will be discussed further in Section 1.4.

These results, for the uniform plane wave case, indicate the sensitivity of macroscopic electromagnetic power absorption to wave polarization. In practice, wave-guiding equipment can be designed that will

produce either the parallel or the perpendicular E-field case. More often, power flows in many directions as is the case in resonant systems, and various wave polarizations exist.

1.3.2.2 Resonant Systems

One of the main reasons that multimode resonant systems, e.g., microwave ovens, are so common, is that EM energy applied to such a resonator tends to 'find' the load, placed within it, rather effectively. Nonetheless, there is a great deal of variability in the performance of such resonant applicators because of the large number of field patterns allowed by the applicator's boundary conditions which are further modified by loading the resonator with a material of variable properties.

Because the theory behind resonant systems is often misunderstood and misused, some of the fundamental relationships involved are briefly reviewed here. As an example, a waveguide of length L is terminated by a short circuit with a reflection coefficient, Γ_1, and the guide is coupled via an iris with reflection coefficient, Γ_2, to a source of EM energy, then the transmitted to incident field ratio is given by [34,35]

$$\frac{\overline{E}_t}{\overline{E}_i} = \frac{1+\Gamma_1}{1-\Gamma_1\Gamma_2 e^{-2\gamma L}} \tag{25}$$

$$\Gamma_1 \cong -1 + j\frac{2X}{Z_o} \tag{26}$$

$$\Gamma_2 = -1 + \frac{2R}{Z_0} \tag{27}$$

where jX is the reactance of the coupling iris and R is the small equivalent resistance of the short circuit plate. For a standard rectangular waveguide, the power in the guide incident on the resonator is related to the incident electric field, $\overline{E}_i$, by

$$P_i = \sqrt{\frac{\varepsilon_o}{\mu_o}}\frac{\lambda}{\lambda_g}\frac{ab}{4}\left|\overline{E}_i\right|^2 \tag{28}$$

where a and b are the waveguide width and height and λ_g is the guide wavelength. Resonance occurs when the denominator of eq. (25) is zero giving rise to very high electric fields in the resonator. It can be shown [35] from these relations that

$$\left|\frac{\overline{E}_t}{\overline{E}_i}\right|^2 = \frac{8}{\pi n}\left(\frac{\lambda}{\lambda_g}\right)^2 \frac{Q_u K}{(K+1)^2} \tag{29}$$

$$Q_u \cong \frac{n\pi}{\frac{R}{Z_o} + \alpha L}\left(\frac{\lambda_g}{\lambda_o}\right)^2 \tag{30}$$

$$K = \frac{\left(\frac{X}{Z_o}\right)^2}{\alpha L + \frac{R}{Z_o}} \tag{31}$$

where α is the empty waveguide's attenuation factor, n is the length of the resonator in half guide wavelengths and K is the coupling factor.

It is not difficult to obtain unloaded Q factors of the order of 5000 at microwave frequencies which translates to an effective localized power gain of 5000. The coupling factor, K, is given directly by the standing wave ratio (or its inverse) on the input line and for critical coupling has the value of unity. Of course, when an absorbing material is present in the resonator, the loaded Q decreases but in most practical applications the field amplification factor (see (29)) is still much larger than unity.

In essence, all resonant systems will enhance the field strength in the material contained in it and the power density relation takes the general form

$$\frac{dP_{abs}}{dV} = k_1 \frac{Q_L \varepsilon'' \left|\overline{E}_i\right|^2}{V} \tag{32}$$

where $\overline{E}_i$ is the field strength of the wave incident on the cavity input and is a constant determined by the resonator type, geometry and coupling arrangement. In high heating rate applications, it is necessary to maintain the resonant frequency and coupling factor constant. This is achieved, for example, by simultaneously controlling the short circuit position and the width of the input coupling iris.

To process larger volumes of material, multiresonant systems are often used which take the form of large rectangular conveyorized microwave tunnels. The easiest way to view the operation of such a system is to consider a plane wave microwave beam entering the resonator and traveling in a straight line till it meets with a reflecting or absorbing object. The waves will reflect from the metallic walls until they meet with an object which will interact with the EM fields to extract their energy. Hence, in a multimode resonant system, energy utilization is usually very good because the waves tend to travel around inside the resonator till the energy is finally absorbed by the process material in

a multipass type of sequence. The microwave feed structure is designed to optimize this effect and to minimize reflected energy to the source.

As a result of the spatial resonant behavior within the oven, the power density will vary as a function of x, y and z which creates temperature extrema in the process material. Part of this undesired temperature variation can be averaged out by passing the material through such a resonant system on a conveyor belt or, in batch type resonators, turntables are used. Another method to average or randomize the waves within the box is to use moving reflectors called mode stirrers.

Microwave to heat conversion efficiencies in multiresonant systems typically range between 50 to 95%. Geometry effects (boundary conditions) due to irregular objects are averaged out because of the randomized nature of the waves incident on the material.

The power density relationships discussed in this section can be used to predict the average field in a mixture which, in turn, can be used in the mixture theory to estimate the localized field strengths at microscopic boundaries as, for example, in an EM sintering process. An example of such a calculation is given in Section 1.4.2.

1.4 Microwave Heating Models

Based on the previous theory, which is simple but surprisingly useful, heating rate formulas can be readily derived. The most useful involves the power density relation given in the previous section as (18). Unfortunately, it is also the equation most easily misapplied by disregarding the underlying assumptions.

1.4.1 Heating Rate Equations

Heat transfer by conduction is governed by the general heat conduction equation which, in rectangular coordinates, for an isotropic rigid solid, is given as

$$\frac{\partial}{\partial x}\left(K\frac{\partial T}{\partial x}\right)+\frac{\partial}{\partial y}\left(K\frac{\partial T}{\partial y}\right)+\frac{\partial}{\partial z}\left(K\frac{\partial T}{\partial z}\right)+q'''=C_p\rho\frac{\partial T}{\partial t} \qquad (33)$$

where q''' represents internal heat generation in watts per unit volume, ρ is the mass density, C_p is the specific heat, K is the variable thermal conductivity, T is the temperature and t is time.

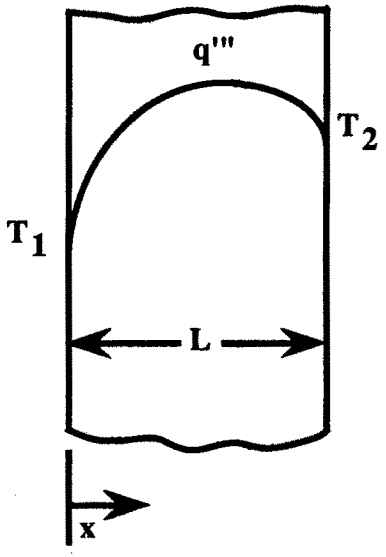

Figure 11.5 Steady state temperature profile for uniform internal heat generation in an infinite but thin slab of thickness L with arbitrary ambient surface temperatures. Assumes constant loss factor and thermal conductivity.

As an example, consider an infinite layer of thickness L being heated with EM energy. Assuming uniform internal heat generation, approximated in the case of low-loss materials in a relatively thin layer, and constant thermal conductivity and loss factor, (33) becomes for steady state conditions

$$\frac{d^2T}{dx^2} + \frac{q'''}{K} = 0 \tag{34}$$

which has the solution [36]

$$T = \frac{q'''}{2K}(Lx - x^2) + \left(\frac{T_2 - T_1}{L}\right)x + T_1 \tag{35}$$

where q''', for a plane EM wave, neglecting interface reflections, is given by

$$\frac{\Delta P_{diss}}{\Delta V} = q''' \cong \frac{\pi f \varepsilon_e'' \left|\overline{E}_{ave}\right|^2}{2} \tag{36}$$

where $\overline{E}_{ave}$ is the average field in the layer. The resulting temperature profile is shown in Fig. 1.5. T1 and T2 are arbitrary surface temperatures set by the ambient conditions. Clearly, this model predicts a temperature maximum inside the material.

An approximation to the heating rate is obtained if heat conduction is totally neglected resulting in

$$q''' = C_p \rho \frac{dT}{dt} \tag{37}$$

For the case of EM heating, q''' is given by (18) and so

$$C_p \rho \frac{dT}{dt} = \frac{dP_{diss}}{dV} = \frac{\pi}{2} f \varepsilon_e'' \left|\overline{E}\right|^2 \tag{38}$$

where $\overline{E}$ is the field strength at the point where the heating rate (dT/dt) is being determined and ε_e'' is the effective loss factor.

The approximate heating rate model described by (38) was used by T. Meek [37] as he sought to model the sintering of ceramics with microwaves. His simple model clearly demonstrated the attributes of EM heating to be conducive to rapid sintering. His model is based on the power density formula, (18), in conjunction with dielectric mixture theory and macroscopic EM boundary conditions. Meek correctly applies the model to a small localized volume in a mixture. Recall that the power density relation, in (18), is a differential relation. Therefore, the electric field and complex permittivity valid at the power calculation point must be used. From the discussion on dielectric mixtures, it is clear that the E-field has different values in the various components of the mixture resulting in different heating rates at different points in the mixture. Meek [37] showed quite clearly that the heating rate in the low-density, unsintered, part of a ceramic mixture is much greater than that of the dense, sintered, part if the following conditions hold:

1. The loss factor of the dense and porous regions are similar.
2. A low density region has a lower permittivity than the high density region (regions may be different materials).

3. Heat conduction, convection, radiation and change of state effects are ignored.

It is interesting to observe from Meek's work that, the change in microwave heating rate, dT/dt, may be a good indicator of how far the sintering process has progressed. Experimental evidence [5, 38] suggests that, once a rapid microwave heating rate has been achieved, a change in dT/dt signals the end phase of the sintering process.

Meek's simple model was based on Maxwell's quasi- static mixture equation. Since quasistatic mixture theory is itself based on the constitutive relations between the EM field quantities, differential heating rate equations can use the electric fields calculated directly from dielectric mixture theory as a later example will show.

A similar but somewhat more complete model of the microwave heating process is given by Palaith et al. [39]. In their case, the power density relation is modified because the authors use a resonant microwave cavity whereas Meek's model assumed plane wave propagation. Moreover, heat loss by radiation is accounted for but thermal diffusion or conduction in the sample is still neglected by assuming a constant internal sample temperature. The heating rate equation is then given by [39]:

$$\rho C_p \frac{dT}{dt} = \frac{0.956 Q P_i \varepsilon''}{V\sqrt{\varepsilon'}} + \frac{0.011 e_w}{h} - 1.35 \times 10^{-12} \frac{e_s}{h}(273 + T)^4 \tag{39}$$

where Q is the quality factor of the loaded cavity (see previous section), P_i is the applied or incident power in J/s, V is the sample volume, e_s and e_w are the sample and wall surface emissivities, C_p is the specific heat capacity, ρ is the mass density, T is the temperature in degrees centigrade, and h is the height of the sample parallel to the E-field. This model, as did Meek's model, neglects the variation of permittivity with temperature. The above equation correlates well with Palaith's experimental data except in the region of maximum heating rate. The second term in the equation accounts for the power absorbed as thermal radiation from the room temperature (298° K) walls containing the sample and is negligibly small in the case of cold (non-insulated) sample containers. If the sample is thermally insulated, the equation can be generalized and becomes

$$\rho C_p \frac{dT}{dt} = k_1 \frac{QP_i}{V} \varepsilon'' + \frac{1.35 \times 10^{-12}}{h} \left[e_w (273 + T_w)^4 - e_s (273 + T_s)^4 \right] \quad (40)$$

where k1 depends on the type of resonator used.

This equation clearly shows the effectiveness of insulating the sample since it will allow partial cancellation of the radiation heat loss term. However, conduction losses are neglected in this model.

In another recent study on the modelling of microwave heating, Watters et al. [40] treat the one-dimensional plane wave problem, assuming constant electrical conductivity (or loss factor) and constant thermal conductivity. Their results show that:

1. The maximum temperature will not occur at the surface if only an internal heat source is assumed, i.e., a non-insulated sample, see, for example, Fig. 1.5.
2. Thermal conductivity is very significant in determining the final temperature profile.

1.4.2 Mixture Theory Applied to Differential Heating

In order to illustrate the usefulness of mixture theory in predicting localized heating rates at the microscopic level, consider a material enclosed in a shell of another material. Such a case is representative of, for example, the ceramic sintering process where grain boundary "shells" surround a crystalline material. One of the few dielectric mixture theories which treat shell inclusions is that of Tinga et al. [4], a brief summary of which is given next. They give equations to predict the internal fields in confocal ellipsoidal inclusions which contain the special cases of spherical shells, ellipsoids, spheres, disks, and needles, shapes typical of those found in material mixtures. Implicit in their solution are the first-order effects of neighboring inclusions, and therefore, their theory approaches the high inclusion-volume limit correctly. Figure 1.6 shows their idealized multiphase mixture. By this choice, their problem reduces to one in which the mixture dielectric constant is determined in a self-consistent manner with the internal fields. By choosing the geometry of V_i, inter-inclusion interactions higher than those of the first order are neglected. However, this is no worse an ap-

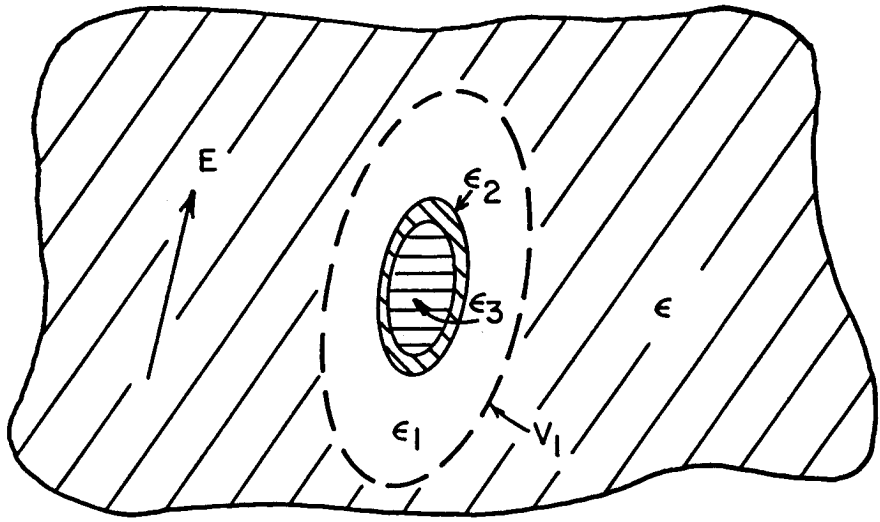

Figure 1.6 Idealized anisotropic multiphase ellipsoidal shell mixture with one shell inclusion shown isolated. After Tinga et al. [4].

proximation than is initially made by specifying a particular geometry and direction for the inclusions.

As an example, consider the special two-phase mixture case of spheres of the inclusion ε_2, or of the host, ε_1, as a function of the volume fraction of the guest. The mixture's dielectric constant, is then given as [4],

$$\frac{\varepsilon - \varepsilon_1}{\varepsilon_1} = \left(\frac{a_2}{a_1}\right)^3 \frac{3(\varepsilon_2 - \varepsilon_1)}{(2\varepsilon_1 + \varepsilon_2) - (a_2/a_1)^3(\varepsilon_2 - \varepsilon_1)} \tag{41}$$

and the field ratio by

$$\frac{\overline{E}_3}{\overline{E}} = \frac{3\varepsilon_1}{(2\varepsilon_1 + \varepsilon_2) - (a_2/a_1)^3(\varepsilon_2 - \varepsilon_1)} \tag{42}$$

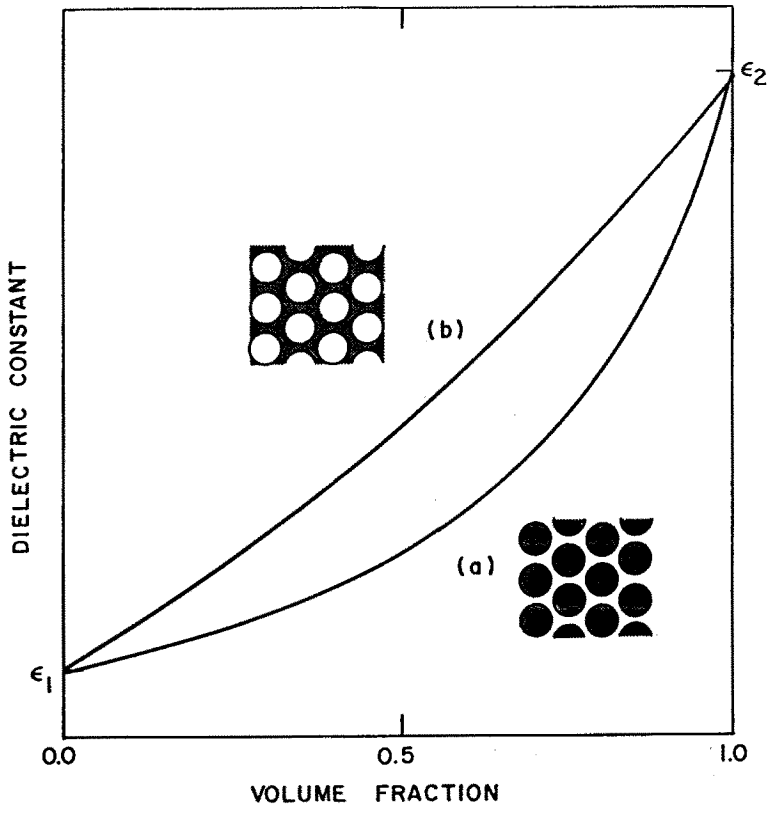

Figure 1.7 Permittivity versus volume loading for spherical shells. $a = \epsilon_1$ "shells surrounding ϵ_2 spheres; $b = \epsilon_2$ "shells" surrounding ϵ_1 spheres.

where a_2 is the radius of the inclusion, ε_2, and a_1 is the equivalent radius of the total mixture volume. A plot of the dielectric constant yields Fig. 1.7 [4]. In case (b), the inclusion acts as a "shell" around the host material.

The solutions to the above multiphase problem are valid for lossless and lossy materials because the boundary conditions to the problem were stated [4] independent of any restrictions on the dielectric constants. In general, mixture equations, are valid for any frequency and temperature if the corresponding values of the individual permittivities are used.

In theoretical modelling work on predicting high-temperature dielectric properties and field strengths, the above multiphase mixture

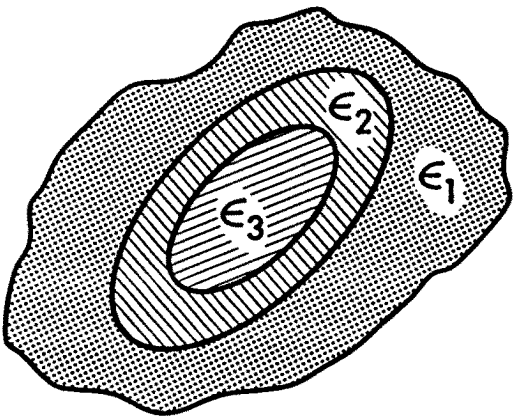

Figure 1.8 Isolated confocal ellipsoidal shell inclusion in a 3 component mixture.

theory is useful since it produces more realistic upper and lower bounds on the dielectric constant and yields a closed-form solution to a reasonably general mixture problem. It should be noted that all mixture theories give worst results when equal amounts of host and guest material are present because of the percolation or particle penetration phenomena. Nevertheless, the following calculations are valid at the local inclusion level.

Consider now an isolated shell such as shown in Fig. 1.8. It can be shown that for such a confocal ellipsoidal shell, the ratio of electric field in the shell to that of the center inclusion is [4]

$$\frac{\overline{E}_2}{\overline{E}_3} = \frac{\varepsilon_2 - n_3(\varepsilon_2 - \varepsilon_3)}{\varepsilon_2 + \frac{(n_2 - n_3)(\varepsilon_2 - \varepsilon_3)(\varepsilon_2 - \varepsilon_1)}{\varepsilon_3 - \varepsilon_1}} \tag{43}$$

where n_2 and n_3 are the depolarization factors of the outer and inner ellipsoids. For very thin shells $(n_2 = n_3)$ this reduces to

$$\frac{\overline{E}_2}{\overline{E}_3} \cong 1 - n_3 + n_3 \frac{\epsilon_3}{\epsilon_2} \tag{44}$$

which for thin spherical shells becomes $(n_3 = 1/3)$

$$\frac{\overline{E}_2}{\overline{E}_3} \cong \frac{2}{3} + \frac{1}{3}\frac{\varepsilon_3}{\varepsilon_2} \tag{45a}$$

and for thin disk shells becomes $(n_3 \cong n_2 = 1)$

$$\frac{\overline{E}_2}{\overline{E}_3} = \frac{\varepsilon_3}{\varepsilon_2} \tag{45b}$$

Similarly, it can be shown using relations from Tinga et al. [4] that the ratio of the average internal shell field to the average field in the mixture for thin disk-like shells is

$$\frac{\overline{E}_2}{\overline{E}_{ave}} = \frac{\varepsilon_1}{\varepsilon_2} \cong \frac{\varepsilon_{eff}}{\varepsilon_{shell}} \tag{45c}$$

Recall from (18) that

$$P_{abs}\alpha\varepsilon_e''|E|^2 \tag{46}$$

Therefore, the ratio of power dissipated in the shell to that in the core is

$$\frac{P_{abs_2}}{P_{abs_3}} \cong \frac{\varepsilon_2''}{\varepsilon_3''}\left|\frac{E_2}{E_3}\right|^2 \tag{47}$$

which for thin disk shells becomes

$$\frac{P_{abs_2}}{P_{abs_3}} \cong \frac{\varepsilon_2''}{\varepsilon_3''}\left|\frac{\varepsilon_3}{\varepsilon_2}\right|^2 \tag{48}$$

combining (48) and (38) gives the approximate heating rate of a thin disk shell,

$$\frac{dT_2}{dt} = \frac{\varepsilon_2''}{\varepsilon_3''}\left(\frac{\varepsilon_3}{\varepsilon_2}\right)^2 \frac{\rho_3}{\rho_2}\frac{C_{P_3}}{C_{P_2}}\frac{dT_3}{dt} \tag{49}$$

It is interesting to note that, since permittivity is proportional to density, the heating rate of the shell is proportional to the cube of the density ratio of the shell and core. As an example, consider an Al_2O_3 inclusion with $\varepsilon_3 = 9$ and a grain boundary or shell with $\varepsilon_2 = 3$. Moreover, because impurities reside at the grain boundary and the Alumina core is crystalline, it follows that the loss factor of the shell is much greater than that of the core, say, for calculation purposes,

$\varepsilon_2''/\varepsilon_3'' = 10$. If we assume the heat capacity ratio to be unity and the density ratio to be 2, the shell to core heating rate ratio becomes

$$\frac{dT_2}{dt} \Big/ \frac{dT_3}{dt} = 180 \tag{50}$$

In the case of a random medium with ellipsoidal inclusions, the local exciting field to average mixture field ratio is

$$\frac{E_L}{E_{ave}} = \frac{\varepsilon}{\varepsilon + N_i(\varepsilon_i - \varepsilon)} \tag{51}$$

where ε is the effective permittivity, ε_i is the inclusion being observed and N_i is the depolarization factor of the inclusion. It is clear from (51) that the local to average field ratio can become very large as would be the case if $\varepsilon_i << \varepsilon$ and N_i approached unity. Equation (51) is used in the derivation of all the effective medium mixture theories. Generalization of (51) for arbitrary particle assemblies and geometries would be beneficial for the study of microscopic microwave sintering and microwave enhanced diffusion studies.

1.5 Temperature and Frequency Dependence of Material Properties

As is evident from all the foregoing, EM heating rates are strong functions of dielectric constant and electric field strength. But both of these quantities depend implicitly on temperature themselves. Therefore, it is appropriate to take a closer look, in particular, at the temperature dependence of the dielectric constant.

1.5.1 Temperature Coefficient of Dielectric Constant

When considering what happens when a material's temperature is raised at constant pressure, one concludes immediately that volume expansion occurs and hence a decrease in the number of polarizable particles per unit volume results. This would give rise to a negative temperature coefficient. On the other had, the polarizability of each particle must increase as temperature is raised due to the availability of a larger volume. According to Bosman and Havinga [41] a third contribution is possible, namely, the dependence of polarizability on

temperature while the volume remains constant. For cubic ionic compounds, they show that the volume dependent part of the temperature coefficient is always positive. This indicates that the macroscopic polarizability increase with temperature is the dominant mechanism in these materials. The three term equation they give is obtained by differentiating the macroscopic Clausius-Mossotti formula with respect to temperature at constant pressure and is restated here for easy reference as

$$\frac{1}{(\varepsilon-1)(\varepsilon+2)}\left(\frac{\partial\varepsilon}{\partial T}\right)_P = -\frac{1}{3V}\left(\frac{\partial V}{\partial T}\right)_P + \frac{V}{\alpha_m}\left(\frac{\partial\alpha_m}{\partial V}\right)_T\left(\frac{1}{3V}\right)\frac{\partial V}{\partial T} + \frac{1}{3\alpha_m}\left(\frac{\partial\alpha_m}{\partial T}\right)_V = A+B+C \tag{52}$$

where α_m is the molar polarizability and V_m the molar volume. Term A is due to the volume expansion causing a decrease in polarizable particles per unit volume. Term B describes the increase in polarizability of a given number of particles as the temperature increases and term C represents the direct dependence of polarizability on temperature at a constant volume. This last term is usually small compared to the first two.

The authors make some interesting observations of relevance to the present discussion. Halides (e.g., KCl, NaCl, LiF) contribute a large volume dependent part to the temperature dependence compared to oxides which have a much smaller volume dependent part due mainly to the large difference in thermal expansion coefficients. They show that the normalized volume dependence of polarizability is

$$\frac{V}{\alpha_m}\left(\frac{\partial\alpha_m}{\partial V}\right)_T = \frac{-B}{A} \tag{53}$$

which is a slowly decreasing function of ε with a value between 2 and 1.

Temperature dependence of the polarizability (term C) is negative for $\varepsilon > 10$ and positive for $\varepsilon < 10$. In the case of ceramics, observed results of $\varepsilon(T)$ indicate positive temperature coefficients [42, 43, 44, 45] and hence one can conclude that the second term is dominant. Since the expansion coefficient is proportional to the dielectric

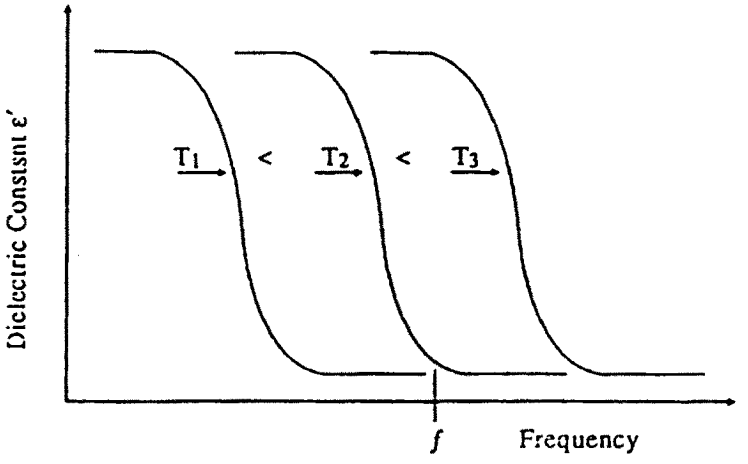

Figure 1.9 Shift in dielectric constant versus frequency curves with temperature variation for materials showing relaxation type of dispersion.

constant's temperature coefficient, the latter can be estimated from the former.

In general, the dielectric constant of ceramic materials shows a relatively linear increase of ε with temperature which is consistent with the above volume dependence of polarizability. The Bosman-Havinga model was applied by Ho [42] and found to give good agreement with permittivity versus temperature measurements on crystalline materials.

1.5.2 Interdependence of Frequency and Temperature Properties

Temperature and frequency dependence of the complex dielectric constant are related and for relaxation type of absorption mechanisms can be shown to be inverse functions. Therefore, if the frequency dependence of a material's permittivity is known, then the temperature variation trend for that material can be estimated. Figures 1.9 and 1.10 illustrate the interrelationship between temperature and frequency dependence.

Using these generic relaxation curves, assuming T2 is room temperature, it is clear that at a given frequency, f, the dielectric constant

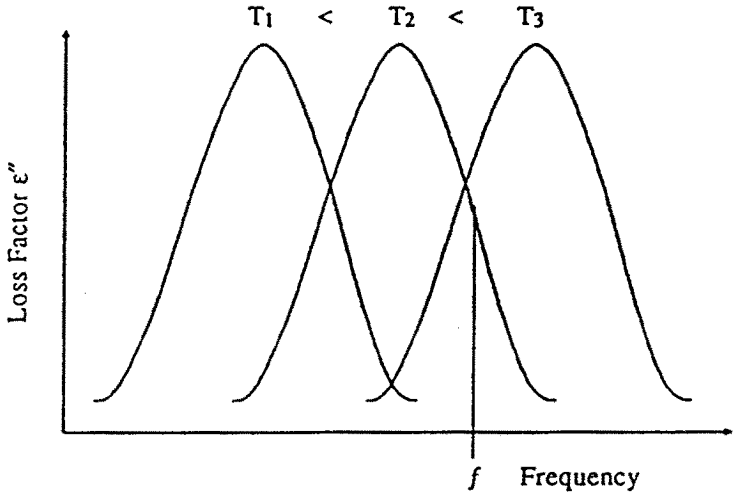

Figure 1.10 Shift in dielectric loss factor versus frequency curves with temperature variation for materials showing relaxation type of dispersion.

will increase with temperature and the loss factor will first increase, pass through a maximum and then decrease again. At high temperatures, the material's conductivity loss, increasing exponentially with temperature, will finally dominate the effective loss factor. A realistic loss factor versus frequency curve is shown in Fig. 1.11 [44]. Bartnikas et al. [46] shows that most loss mechanisms will exhibit some type of relaxation behavior as shown above.

Conductivity, which is proportional to mobility, is strongly temperature dependent and can be written as

$$\sigma = \sigma_o e^{-\frac{E}{kT}} \tag{54}$$

where E is an activation energy. From comparisons between different ceramic materials [45] it is apparent that impurities significantly affect the conductivity and the dielectric loss factor. Impurities often enhance the conduction mechanism by reducing the energy gap between the valence and conduction bands. In fact, impurities can be purposely introduced into a material to increase the effective heating rate. Note, however, that impurities may also affect the final product quality adversely. Moreover, the effective energy penetration decreases

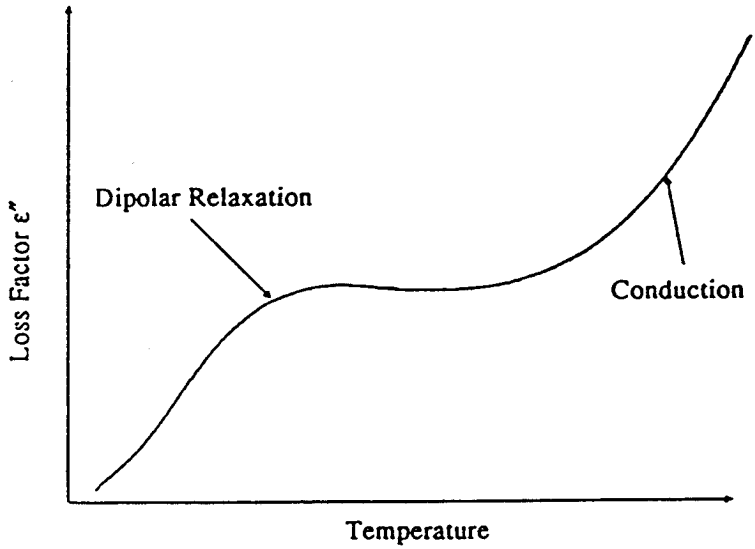

Figure 1.11 Loss factor as a function of temperature showing a relaxation region overlapped by high temperature conductivity losses. Typical of ceramic oxides, e.g., CuO, ZnO [41, 42].

as losses increase, opposing the usual goal of uniform heating. On the other hand, thermal conductivity may vary considerably and will play a significant role in determining the final heating profile.

Many materials with very low loss factors at lower temperatures exhibit rapidly increasing losses at higher temperatures due to the exponential dependence of conductivity on temperature and possibly other phenomena, such as phase transitions [43, 44]. This means that preheating of such materials by some means is necessary before EM heating can become effective. In ceramic processing, sintering aids, which have reasonable low temperature losses and which will burn off before final sintering, may be one solution to the preheating problem.

All of this means that data on the temperature variation of material properties need to be available before a good EM heating process can be designed. Microwave dielectric and magnetic properties can be measured using a host of different methods. To measure them at very high temperatures is difficult but Frost [47, 48] and others [49, 50, 51] have developed different techniques such as free space absorption, resonant cavity, and waveguide absorption methods which can measure dielectric properties up to 1500° C. It is, however, often difficult to de-

embed the true material properties from the system parameters being measured.

1.6 Other Microwave Field Effects

1.6.1 Microwave Enhanced Diffusion

Does the use of microwave energy enhance diffusion? There appears to be experimental evidence that this is so. Gibson et al [52] argue that active disruption of molecular bonding takes place when polymeric materials are heated with microwaves. This results in an increased proportion of mobile diffusant molecules and hence in an increased value of the diffusion coefficient. They suggest that this effect may be a general one and one which is different from a plain Joule heating effect.

In ceramic fusing applications, Meek [38] and others [39, 40] have given evidence of the fact that diffusion while heating with microwaves is enhanced. Very rapid joining of ceramics with or without binding phases has been achieved resulting in nearly invisible joints (microscopically). One author attributes the results of Meek to preferential grain-boundary heating and the melting of a glassy boundary phase [42]. Enhanced diffusion and preferential grain-boundary heating, predicted by dielectric mixture theory, may well be related to the same physical cause of local field enhancement and energy concentration as discussed earlier.

Recently [53], some significant evidence was presented indicating a greatly reduced activation energy of 170 kJ/mole for the microwave, as compared to 575 kJ/mole for the conventional sintering process. This was calculated from a plot of sintering rates versus inverse temperature. Microwave annealing was also shown to possess a reduced activation energy of 480 kJ/mole compared to the conventional 630 kJ/mole. They conclude that the boundary or volume diffusion constant is higher for the microwave than for the conventional heating process which is also consistent with the enhanced grain boundary heating prediction.

1.6.2 High Field Intensity Problems

High power or high field intensity effects exhibit themselves main ly in the form of arcing or plasma formation. The polarization behavior

of most materials remains linear for all practical proposes up to very high field strengths. Breakdown due to ionization occurs quite readily in resonant systems [54, 55] and is often observed in microwave ovens [56]. Ionization can be initiated by charge buildup on highly conducting surfaces or by geometry dependent polarization mechanisms which cause field enhancement. Prevention of dielectric breakdown is not always readily achievable. On the other hand, purposely generating the breakdown to cause plasma formation has been the basis for many unique applications in the chemical, ceramic and electronic industries such as plasma etching, destruction of toxic materials and high speed sintering operations [57, 58].

1.7 Conclusions

Dielectric mixture theory for heterogeneous materials was review ed to emphasize its importance in modelling high power electromagnetic field interactions with materials. The popular concept of treating materials as having an effective permittivity was shown to be a valid approximation whenever the characteristic dimensions of the mixture inclusions are much less than the EM wavelength and when percolation phenomena can be ignored. EM energy absorption equations and macroscopic boundary conditions were found to set important constraints on an EM heating system. Microwave heating models were derived to allow heating rate predictions to be made at both the macroscopic and localized microscopic levels with the help of mixture theory. Applying the results, strong differential heating was shown to be possible in certain situations underlining the fact that mixture theory can be a very useful tool in predicting energy dissipation in a material.

The importance and interdependence of a material's frequency and temperature properties was reviewed emphasizing the observation that, at very high temperatures, the conduction loss mechanism tends to dominate all others. Finally some experimental facts indicating EM enhancement of diffusion were presented.

References

[1] Maxwell, J. C., *A Treatise on Electricity and Magnetism*, **1,2** 3rd ed. 1891, Dover Publication Inc., 1954.

[2] Van Beek, L. K. H., "Dielectric behavior of heterogeneous systems," *Progress in Dielectrics*, **7**, 69–114, Heywood and Company Ltd., London, 1967.

[3] Tinga, W. R., "Multiphase Dielectric Theory-Applied to Cellulose Mixtures," Ph.D. Thesis, University of Alberta, Edmonton, Alberta, Canada, 1969.

[4] Tinga, W. R., W. A. G. Voss, and D. F. Blossey, "Generalized approach to multiphase dielectric mixture theory," *J. of Appl. Phys.*, **44(9)**, 3897–3902, 1973.

[5] Sihvola, A., "Analysis of Microwave Structures and Mixing Formulae with Application to Remote Sensing Measurements," Ph.D. Thesis, Helsinki University of Technology, 1986.

[6] Sihvola, A., and J. A. Kong, "Effective permittivity of dielectric mixtures," *IEEE Trans.* **GE–26(4)**, 420–429, 1988.

[7] De Loor, G. P., "Dielectric Properties of Heterogeneous Mixtures," Ph.D. Thesis, Leiden, The Netherlands, 1956.

[8] Kraszewski, A., "Prediction of the dielectric properties of two-phase mixtures," *J. Microwave Power*, **12**, 215–222, 1977.

[9] Sihvola, A., see elsewhere in this book.

[10] Varadan, V. K., Y. Ma, A. Lahktakia, and V. V. Varadan, "Microwave sintering of ceramics:," *Mat. Res. Soc. Symp. Proc.*, **124**, 45–57, 1988.

[11] Böttcher, C. J. F., *Theory of Electric Polarisation*, Elsevier Publishing Co., New York, 1952.

[12] Yaghjian, A. D., "Electric dyadic Green's Functions in the source region," *Proc. IEEE*, **68(2)**, 248–263, 1980.

[13] Lord Rayleigh, "On the influence of obstacles arranged in rectangular order upon the properties of a medium," *Philosophical Magazine*, **32**, 481–502, 1892.

[14] Cohen, R. W., G. D. Cody, M. D. Coutts, and B. Abele, "Optical

properties of granular silver and gold films," *Phys. Rev. B*, **8(8)**, 3689–3701, 1973.

[15] Wiener, O., *Abh. Math. Phys. Kl. Sachs Akad. Wiss.*, Leipzig, **32**, 509, 1912.

[16] Bruggeman, D. A. G., "Berechnung Verschiedener Physikalischer Konstanten von Heterogenen Substanzen," *Annalen der Physik*, **24**, 636–644, 1935.

[17] Niesel, W., *Ann. Phys.* (Leipz.) **10**, 336, 1952.

[18] Looyenga, H., "Dielectric constants of mixtures," *Physica*, **321**, 401–406, 1965.

[19] Wait, J. R., *Electromagnetic Wave Theory*, Harper and Row, Ch. 2, 54–75, 1985.

[20] Stroud, D., "Generalized effective-medium approach to the conductivity of an inhomogeneous material," *Phys. Rev. B*, 12(8), 3368–3373, 1975.

[21] Brown, W. F., Jr., "Solid mixture permittivities," *J. of Chemical Physics*, **23(8)**, 1514–1517, 1955.

[22] Nelson, S. O., "Method for determining dielectric properties of solids from measurements on pulverized materials," *1987 IEEE MTT-S Int. Microwave Symp. Digest*, **1** 461–463, 1987.

[23] Nelson, S. O., see chapter in this book.

[24] Lewin, L., "The electrical constants of a material loaded with spherical particles," *Proc. IEE*, **94**, Part 3, 65–68, 1947.

[25] Lichtenecker, K., *Kolloid-Beih.*, **23**, 285, 1926.

[26] Onsager, L., *J., Amer. Chem. Soc.*, **58**, 1486, 1936.

[27] Polder, D., and J. H. van Santen, "The effective permeability of mixtures and solids," *Physica XII*, **5**, 257–271, 1946.

[28] Taylor, L. S., "Dielectrics loaded with anisotropic materials," *IEEE Trans.*, **AP-14**, 669–670, 1966.

[29] Korneenko, I. A., "Mean values of the parameters in inhomogeneous media," *Soviet Physics – Technical Physics*, **5**, 40, 1960.

[30] Franck, V., "On the penetration of a static homogeneous field in an anisotropic medium into an ellipsoidal inclusion consisting of

another anisotropic medium," *Symp. on Electromagnetic Theory and Antennas*, Oxford Pergamon, London, 615–623, 1962.

[31] Kirkwood, J. G., "On the theory of dielectric polarization," *J. of Chemical Physics*, **4**, 592–601, 1936.

[32] Tsang, L., and J. A. Kong, "Scattering of electromagnetic waves from random media with strong permittivity fluctuations", *Radio Science 16(3)*, 303–320, 1981.

[33] Sheng, P., *Phys. Rev. Lett. 45*, 60 (1980).

[34] Collin, R. E., *Foundations of Microwave Engineering*, McGraw Hill, 1966.

[35] Thiebaut, J. M., J. F. Rochas, M. Manoury, and G. Roussy, "Control of the fields and hysteresis heating process in a microwave resonant applicator," *J. of Microwave Power*, **17(3)**, 187–194, 1982.

[36] *The Essentials of Heat Transfer I*, Research and Education Association, New York, 1987.

[37] Meek, T. T., "Proposed model for the sintering of a dielectric in a microwave field," *J. Mat. Science Letters (6)*, 638–640, 1987.

[38] Meek, T. T., "Ceramic-Ceramic seals by microwave heating," *J. Mat. Science Letters (5)*, 270–274, 1986.

[39] Palaith, D., R. Silberglitt, C. C. M. Wu, R. Kleiner, and E. L. Libelo, "Microwave joining of ceramics," *Mat. Res. Soc. Symp. Proc. (24)*, 255–266, 1988.

[40] Watters, D. G., M. E. Brodwin, and G. A. Kriegsman, "Dynamic temperature profiles for a uniformly illuminated planar surface," *Mat. Res. Soc. Symp. Proc. (24)*, 129–134, 1988.

[41] Bosman, A. J., and E. E. Havinga, "Temperature dependence of Dielectric constants of cubic ionic compounds," *Physical Review*, **129(4)**, 1593–1600, 1963.

[42] Ho, W. W., "High-temperature dielectric properties of polycrystalline ceramics," *Materials Research Society, 1988 Symp. Proc. Microwave Processing of Materials*, **124**, 137–148, 1988.

[43] Tinga, W. R., "Microwave dielectric constants of metal oxides at high temperatures: Part I," *Electromagnetic Energy Reviews*, **1(5)**, 1–6, 1988.

[44] Tinga, W. R., "Microwave dielectric constants of metal oxides at high temperatures: Part II," *Electromagnetic Energy Reviews, 2(1)*, 1–6, 1989.

[45] Westphal, W. B., and A. Sils, "Dielectric Constants and Loss Data," Airforce Materials Laboratory, Wright Patterson Airforce Base, Ohio, Techn. Rept. **AFML-TR-72-39**, 1972.

[46] Bartnikas, R., and R. M. Eichhorn, "Engineering Dielectrics, Volume IIA, Electrical Properties of Solid Insulating Materials: Molecular Structure and Electrical Behavior," *ASTM Special Techn. Publication 783*, March 1983.

[47] Frost, H. M., "Capability for Measuring Millimeter-Wave Dielectric Properties in Free Space and at Elevated Temperatures," DOE DAFS/ADIP/SPM Semi-annual Progress Report on Fusion Reactor Materials, Los Alamos National Laboratory (**LA-UR-86-4226**), 1986.

[48] Frost, H. M., "Dielectric properties of ceramics," *Materials Science and Technology Review 1986.*

[49] Bosisio, R. G., R. Dallaire, and P. Phromothansy, "A non contact temperature monitor for the automatic control of microwave ovens," *J. of Microwave Power*, **12(4)**, 309–317, 1977.

[50] Araneta, J. C., M. Brodwin, and G. E. Kriegsmann, "High-temperature microwave characterization of dielectric rods," *IEEE Trans.*, **MTT 32(10)**, 1328–1335, 1984.

[51] Wong, D. K., "Microwave Dielectric Constants of Metal Oxides at High Temperatures," M.Sc. Thesis, University of Alberta, Edmonton, Canada, 1975.

[52] Gibson, C., I. Mathews, and A. Samuel, "Microwave enhanced diffusion in polymeric materials," *J. of Microwave Power and Electromagnetic Energy*, **23(1)**, 17–28, 1988.

[53] Janney, M. A., H. D. Kimrey, and M. A. Schmidt, "Grain growth in microwave-annealed alumina," American Ceramics Society, 99th Annual Meeting Symp. IX: Symp. on Microwave Processing of Ceramics, April, 1989.

[54] McDonald, A. A., *Microwave Breakdown in Gases*, Wiley, 1966.

[55] Johnson, D. L., and M. E. Brodwin, EPRI Research Project 2730–

01, Interim Report, March 1987.

[56] Ishii, T. K., "Theoretical analysis of arcing structure in microwave ovens," *J. of Microwave Power*, **18(4)**, 337–344, 1983.

[57] Asmussen, J., and R. Garard, "Precision microwave applicators and systems for plasma and material processing," *Mat. Res. Soc. Symp. Proc.*, **124**, 347–352, 1988.

[58] Salsman, J. B., and R. H. Church, "The rapid formation of tungsten carbide in a microwave induced plasma," American Ceramics Society, 99th Annual Meeting Symp. IX: Symp. on Microwave Processing of Ceramics, April, 1989.